Spontaneous-fission half-lives of deformed superheavy nuclei

R. Smolańczuk, J. Skalski, and A. Sobiczewski
Soltan Institute for Nuclear Studies, Hoza 69, PL-00-681 Warszawa, Poland
and Gesellschaft für Schwerionenforschung, D-64220 Darmstadt, Germany
(Received 9 August 1994)

Spontaneous-fission half-lives of the heaviest nuclei are analyzed in a multidimensional deformation space. They are calculated in a dynamical approach, without any adjustable parameters. The potential energy is obtained by the macroscopic-microscopic method and the inertia tensor by the cranking method. The action integral is minimized by a variational procedure. Even-even nuclei with proton number $Z=104-114$ and neutron number $N=142-176$ are considered. The results reproduce existing experimental data rather well. Relatively long half-lives are predicted for many unknown nuclei, sufficient to detect them if synthesized in a laboratory.

PACS number(s): 25.85.Ca, 21.10.Tg, 24.75.+i, 27.90.+b

I. INTRODUCTION

The objective of this paper is to analyze spontaneous-fission properties of deformed superheavy nuclei in a multidimensional deformation space. Such quantities as the potential energy (in particular the potential-energy barrier along the fission trajectory), the effective inertia along the fission trajectory, and the fission half-life of a nucleus are studied. Even-even nuclei with proton number $Z=104-114$ and neutron number $N=142-176$ are considered.

By deformed superheavy nuclei, we understand nuclei situated in the neighborhood of the nucleus $^{270}108$ (^{270}Hs), which is expected to be a doubly magic deformed nucleus [1,2]. One specific property of these nuclei is that they are expected to be well deformed (e.g., [2]). Consequently, and in contrast to spherical or nearly spherical nuclei, we need a sufficiently large deformation space to calculate even the ground-state (equilibrium) energy of a nucleus. Another property is that the fission barriers of these very heavy nuclei are relatively simple and thin. The deformation space required for the analysis of such barriers is much smaller than the space required for lighter nuclei, like those with $Z=92-102$, which have much thicker and more complex barriers. In practice, the space used to analyze the ground state of the nuclei considered is sufficient also to investigate their fission barriers. A third property is that shell effects are extremely important for these nuclei. Most, or may be even all, of them would not exist without these effects [3,2]. This puts a strong requirement on theory to account for these effects as accurately as possible, both in the potential energy and in the inertia of a nucleus with respect to the fission mode.

Being a region of very heavy nuclei, it still contains a number of nuclei with measured fission half-lives. These provide a test for the calculations.

Our present analysis belongs to a series of papers [4–6], treating the spontaneous fission in a dynamical way, i.e., taking into account the inertia tensor of a nucleus, when looking for the trajectory with the highest probability of barrier penetration. In older papers [4,5], a rather poor, two-dimensional deformation space was taken. More particularly, only deformations of the lowest multipolarities: quadrupole, β_2 (or ϵ_2), and octupole, β_3 (or ϵ_3), have been considered. Deformations of higher multipolarities have been taken into account only in a very approximate way. In a more recent analysis [6], a four-dimensional space, $\{\beta_\lambda\}$, $\lambda=2,3,4,5$, was used. Only a space of such dimension can be used presently, for computational reasons. In the present paper, also a four-dimensional space is taken, but this is another space, appropriate for very heavy nuclei considered here. This space $\{\beta_\lambda\}$, $\lambda=2,4,6,8$, disregards the odd-multipolarity deformations β_3 and β_5, which are important for lighter nuclei with thicker and more complex fission barriers considered in [6], but are unimportant for very heavy nuclei with thin and relatively simple barriers described here. Instead of β_3 and β_5, the space includes the higher-multipolarity deformations β_6 and β_8, which are important for the heaviest nuclei for proper description of their shell effects.

An advantage of the dynamical analysis is that no adjustable parameters are used. In statical considerations [7–11], a phenomenological inertia function is taken, which has at least one free parameter fitted to experimental data. Additionally, the phenomenological function disregards the shell structure of a nucleus. This structure, which is extremely important for the considered nuclei, is taken into account in the microscopic inertia tensor used in the dynamical approach.

The present theoretical paper is closely connected with the intensive experimental activity on the synthesis and study of the properties of heaviest nuclei of recent years (cf., e.g., [12–19]). It aims at the interpretation of existing data and in predictions of properties of yet unknown nuclei.

Some of the results of this paper have been presented earlier [20–22].

The method of the analysis is described in Sec. II, the results and discussion are given in Sec. III, and conclusions drawn from the study are presented in Sec. IV.

II. METHOD OF THE CALCULATIONS

A. Potential energy

The potential energy of a nucleus is calculated in a macroscopic-microscopic approach. The Yukawa-plus-

exponential model [23] with the standard values of its parameters (e.g., [24]) is used for the macroscopic part of the energy. The Strutinski shell correction, based on the Woods-Saxon single-particle potential [25], is taken for the microscopic part. The "universal" variant of the parameters of the potential is chosen (the same as in [2] where they are also specified).

The residual pairing interaction is treated in the usual BCS approximation. The strength of the interaction is taken the same as in [2], where it has been fitted to recent data for nuclear masses.

B. Inertia tensor

The inertia tensor describes the inertia of a nucleus with respect to changes of its deformation. We calculate it in the cranking approximation. The corresponding formula is (e.g., [26–28,5])

$$B_{\alpha_i\alpha_j}=2\hbar^2\sum_{\nu\nu'}\frac{\langle\nu|\partial H/\partial\alpha_i|\nu'\rangle\langle\nu'|\partial H/\partial\alpha_j|\nu\rangle}{(E_\nu+E_{\nu'})^3}(u_\nu v_{\nu'}+u_{\nu'}v_\nu)^2+P^{ij}, \tag{1}$$

where α_i and α_j are the deformation parameters, H is the single-particle Hamiltonian, u_ν and v_ν are the BCS variational parameters, and E_ν is the quasiparticle energy corresponding to the single-particle state $|\nu\rangle$. The term P^{ij} describes the effect of the collective motion on the pairing interaction. Various properties of the tensor $B_{\alpha_i\alpha_j}$ have been discussed in [26–29,5].

The inertia tensor provides a metric in deformation space, when calculating the penetration of a nucleus through the fission barrier.

C. Spontaneous-fission half-life

The spontaneous-fission half-life $T_{\rm sf}$ is calculated by the formula

$$T_{\rm sf}=T_0P^{-1}, \tag{2}$$

where P is the probability of the barrier penetration by a nucleus and T_0 is the half-life when this probability is equal to unity. The half-life T_0 is determined by the number of assaults of a nucleus on the fission barrier in unit time, $\omega_0/2\pi$,

$$T_0=2\pi\ln 2/\omega_0, \tag{3}$$

and, thus, by the zero-point vibration energy of the nucleus in the fission degree of freedom, $E_{\rm zp}=0.5\hbar\omega_0$.

The probability P is obtained in the semiclassical (WKB) approximation

$$P=[1+\exp 2S(L)]^{-1}, \tag{4}$$

where the action integral $S(L)$ along a one-dimensional trajectory L in a multidimensional deformation space is

$$S(L)=\int_{s_1}^{s_2}\left\{\frac{2}{\hbar^2}B_L(s)[E_L(s)-E_0]\right\}^{1/2}ds. \tag{5}$$

Here, $E_L(s)$ is the potential energy, $B_L(s)$ is the effective inertia, both along the trajectory L, and E_0 is the energy of a fissioning nucleus. The parameter s specifies the position of a point on the trajectory L, with s_1 and s_2 corresponding to the entrance and exit points of the barrier, i.e., to the classical turning points determined by $E_L(s)=E_0$. The effective inertia $B_L(s)$ associated with the fission motion along the trajectory L is

$$B\equiv B_L(s)=\sum_{ij}B_{\alpha_i\alpha_j}(s)\frac{d\alpha_i}{ds}\frac{d\alpha_j}{ds}, \tag{6}$$

where $B_{\alpha_i\alpha_j}$ are components of the inertia tensor, Eq. (1), and α_i, α_j are the deformation parameters (β_λ).

The half-life $T_{\rm sf}$ is calculated in the dynamical way (e.g., [30,5]), i.e., along the dynamical trajectory $L_{\rm dyn}$, for which the action integral $S(L)$ is minimal, with full dependence of the inertia tensor $B_{\alpha_i\alpha_j}$ on the deformation taken into account.

D. Deformation space

Axially symmetric shapes are used in our analysis of spontaneous fission. These shapes are described by the usual deformation parameters β_λ, appearing in the expression for nuclear radius (in the intrinsic frame of reference) in terms of spherical harmonics $Y_{\lambda 0}(\vartheta)$,

$$R(\vartheta)=R_0(\beta_\mu)\left[1+\sum_\lambda\beta_\lambda Y_{\lambda 0}(\vartheta)\right], \tag{7}$$

where the dependence of R_0 on β_μ is determined by the volume-conservation condition.

The reason to disregard the axially asymmetric shapes is based on the dynamical treatment of fission. Along the static

trajectory (i.e., the trajectory along which the potential enegy is minimal), the potential energy is usually decreased by the nonaxial (γ) deformation by up to about 1 MeV [31,4,32]. The effective inertia B, Eq. (6), is, however, large along this trajectory and leads to a larger action integral than the integral along the trajectory with $\gamma=0$. This has been directly shown in [32] for the nucleus $^{260}106$ (^{260}Sg), belonging to the region considered here, and in [4] for a lighter nucleus.

Concerning the axial deformations β_λ, we find, similar to [33], that it is sufficient to consider the deformations of multipolarities up to $\lambda=8$. The contributions of β_9 and β_{10} to the potential energy are already negligible. The deformations with odd multipolarities $\lambda=3,5,7$ are not important because they contribute to the energy only behind the thin fission barriers of these very heavy nuclei, considered here. Thus, the potential energy is analyzed in four-dimensional deformation space $\{\beta_\lambda\}$, $\lambda=2,4,6,8$.

E. Details of the calculations

The potential energy E and the inertia tensor $B_{\beta_\lambda\beta_\mu}$, Eq. (1), are calculated individually for each nucleus. No averaging over proton Z and neutron N numbers is used.

The potential energy E is calculated at grid points (β_2,β_4) with steps $\Delta\beta_2=\Delta\beta_4=0.05$. The range of both β_2 and β_4 is taken individually for each nucleus, to obtain the whole region of the fission barrier.

The dynamical calculations of T_{sf} are performed in the approximation tested in [32]. These are the calculations performed in two-dimensional deformation space $\{\beta_\lambda\}$, $\lambda=2,4$, but with the potential energy E minimized at each point (β_2,β_4) of this space in the remaining degrees of freedom: β_6 and β_8. Thus, the potential energy and, correspondingly, the inertia tensor are

$$E(\beta_2,\beta_4;\beta_\nu^m),\quad B_{\beta_\lambda\beta_\mu}(\beta_2,\beta_4;\beta_\nu^m), \tag{8}$$

where β_ν^m, $\nu=6,8$, is the value of β_ν, at which the energy E is minimal at the point (β_2,β_4). A detailed study [32] of dynamics in deformation spaces of various dimensions has shown that this approximation is rather good for nuclei considered in this work.

To obtain a sufficiently accurate fission trajectory, the values of the potential energy E and of the inertia tensor $B_{\beta_\lambda\beta_\mu}$ of Eq. (8) are interpolated (by the standard procedure SPLIN3 of the IMSL library) to the more dense grid $\Delta\beta_2=0.01,\Delta\beta_4=0.0025$. Only on such a dense grid has the variational calculation been performed, using a dynamical-programming method described in [5].

To calculate the ground-state energy E_0 of a nucleus [Eq. (5)],

$$E_0=E(\beta_\lambda^0)+E_{zp}, \tag{9}$$

the zero-point energy in the fission degree of freedom is taken as $E_{zp}=0.7$ MeV. This is the value close to that calculated in [2]. Here, $E(\beta_\lambda^0)$ is the value of the potential energy at the equilibrium (ground-state) deformation β_λ^0. The energy E_{zp} determines simultaneously the number of assaults of a nucleus on the fission barrier, according to Eq. (3).

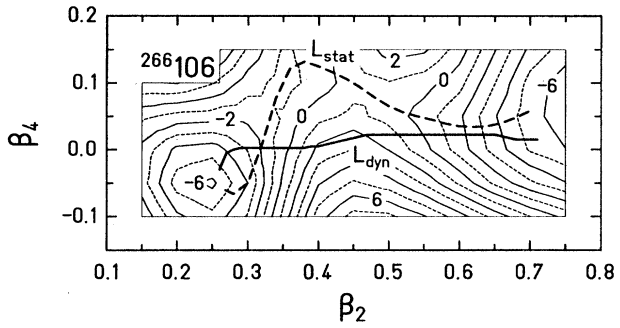

FIG. 1. Contour map of the potential energy E calculated as a function of the deformations β_2 and β_4, for the nucleus $^{266}106$ (^{266}Sg). At each point (β_2,β_4), the energy is minimized in β_6 and β_8 degrees of freedom. Numbers at the contour lines give the values of the energy in MeV. The energy difference between neighboring solid lines is 2 MeV. Dashed lines divide this difference by two. Dynamical, L_{dyn}, and statical, L_{stat}, fission trajectories are shown.

III. RESULTS AND DISCUSSION

A. Potential energy and fission trajectory

Figure 1 illustrates a map of the potential energy. As an example, we take the recently synthesized [17,18] nucleus $^{266}106$ (^{266}Sg). Among all observed even-even nuclei, it is closest to the predicted [1,2] doubly magic deformed nucleus $^{270}108$ (^{270}Hs). Because of its relatively long half-life, it is also the isotope of the element 106 (Sg) by which the chemical properties of this element are planned to be studied [34]. At each point (β_2,β_4), the energy is minimized in the β_6 and the β_8 degrees of freedom. The dynamical fission trajectory L_{dyn} is also shown in Fig. 1. It has a tendency to be close to a straight line and to have a possible small slope with respect to the β_2 axis, as both these features lead to a small effective inertia B, Eq. (6), along the trajectory and, consequently, to a small action integral. According to Eq. (6), the small slope corresponds to a small contribution of the components $B_{\beta_\lambda\beta_\mu}$ of the inertia tensor with $\lambda,\mu>2$ to B. A large curvature or a large slope of the dynamical trajectory may appear only at the beginning or at the end of the barrier, where the potential energy is small and a large value of B is less important.

The static trajectory L_{stat} is also shown in Fig. 1, for comparison. The effective inertia B is usually large along this trajectory, as discussed in [32], and, in spite of a smaller fission barrier, leads to a larger action integral than that along the dynamical trajectory.

B. Fission barrier

The shape of the fission barrier calculated along the dynamical trajectory L_{dyn} is illustrated in Fig. 2. One can see that the barrier is thin. It ends at a deformation $\beta_2\approx0.7$, thus at about the deformations of fission isomers, i.e., the defor-

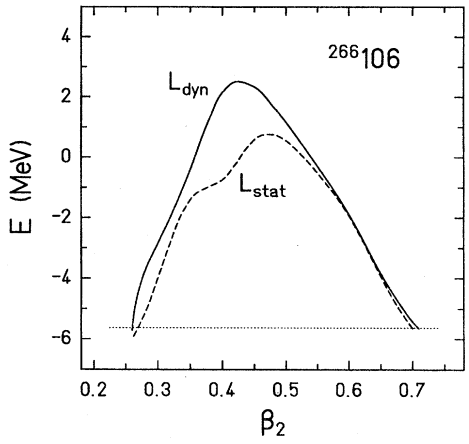

FIG. 2. Shape of the potential-energy barrier calculated along the dynamical and statical fission trajectories, for the nucleus $^{266}106$.

mations at which the second minimum in energy appears for lighter nuclei, around americium. The barrier is, however, high. This is mainly due to a large (in absolute value), negative shell correction $E_{\rm sh}$ to the ground-state energy. For the considered nucleus $^{266}106$, the correction is $E_{\rm sh}=-6.3$ MeV.

The (static) barrier, calculated along the static trajectory $L_{\rm stat}$, is also shown in Fig. 2, for comparison. This barrier is important for calculations of the competition between neutron emission and fission (Γ_n/Γ_f) of an excited nucleus.

One can see in Fig. 2 that the static barrier is lower by almost 2 MeV and it is also different in shape from the dynamical barrier. The height of the statical barrier is about equal to the ground-state shell correction $E_{\rm sh}$, as there is almost no contribution of the smooth part of the energy to this height, and the shell correction at the saddle point is rather small, as discussed in [3].

Figure 3 shows a contour map of the height of the dynamical fission barrier $B_f^{\rm dyn}$. As mentioned above, the height is large. It is larger than 7 MeV for about 20 of the nuclei considered. The largest value, 8.8 MeV, is obtained for the nucleus $^{268}106$, i.e., the nucleus with the neutron number $N=162$, corresponding to the predicted closed deformed neutron shell.

A contour map of the height of the static fission barrier $B_f^{\rm stat}$ is given in Fig. 4. One can see that Fig. 4 presents a "mountain," which is flattened to some degree with respect

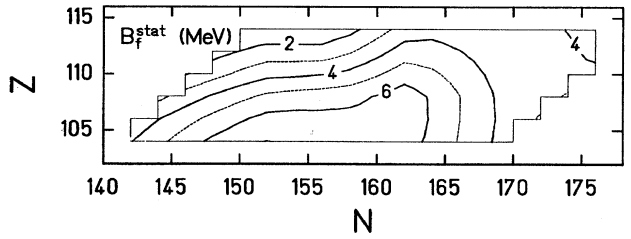

FIG. 4. Same as in Fig. 3, but for the static fission barrier $B_f^{\rm stat}$.

to the "mountain" of $B_f^{\rm dyn}$ (Fig. 3). It is decreased around the top (by up to about 2 MeV), while it remains almost unchanged at the bottom, in comparison with $B_f^{\rm dyn}$.

As the ground-state shell correction $E_{\rm sh}$ is the main contribution to the barrier heights $B_f^{\rm dyn}$ and $B_f^{\rm stat}$, it is interesting to look also at the map of $E_{\rm sh}$. This is shown in Fig. 5. One can see a really strong correlation between the three maps.

It is worth noting in Fig. 5 that, when moving from lighter to heavier nuclei, after the maximum (in absolute value) of $E_{\rm sh}$, obtained for the predicted doubly magic deformed nucleus $^{270}108$, one observes a minimum of this quantity for $N\approx 170$ and then one sees its increase again, when approaching the predicted doubly magic spherical nucleus $^{298}114$. The corresponding behavior is also observed in the fission-barrier heights in Fig. 3 and Fig. 4.

C. Effective inertia

The effective inertia B, Eq. (6), calculated along the dynamical fission trajectory $L_{\rm dyn}$ is shown in Fig. 6. One can see that it is a rather strongly fluctuating function of deformation. This is because the inertia tensor (mass parameters) is a much less collective quantity than the potential energy or even the moment of inertia (i.e., the inertia of a nucleus with respect to its rotation) as was discussed in detail in [28]. Thus, it is very sensitive to the internal, single-particle structure of a nucleus which changes with its deformation. A general tendency is that the inertia tensor is small at deformations at which the potential energy has deep minima (low single-particle-level density at the Fermi level at these deformations) and large at deformations at which the potential energy has particularly large values, e.g., maxima or saddle points (high single-particle-level density at these points).

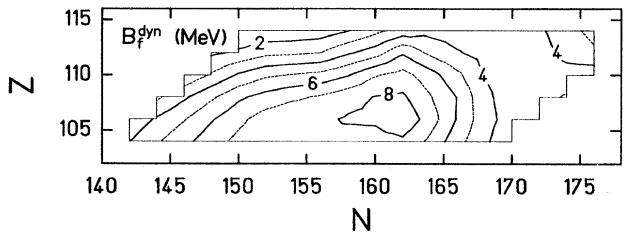

FIG. 3. Contour map of the height of the dynamical fission barrier, $B_f^{\rm dyn}$, plotted as a function of the proton Z and neutron N numbers.

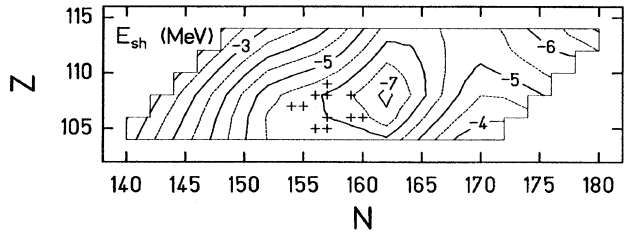

FIG. 5. Contour map of the ground-state shell correction, $E_{\rm sh}$, to the potential energy E. Crosses indicate the heaviest nuclei synthesized up to now.

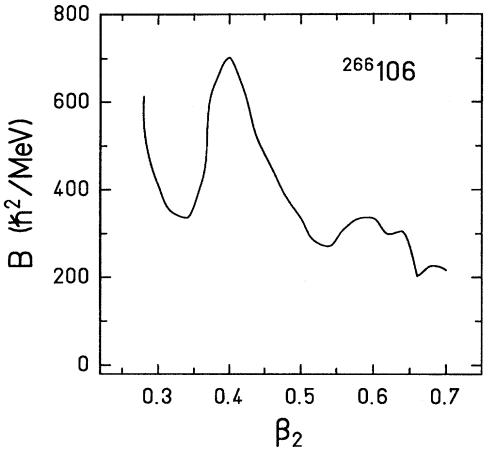

FIG. 6. Effective inertia B calculated along the dynamical fission trajectory, for the nucleus ^{266}106.

This means that the regions around the maxima in the potential energy along the fission trajectory should be especially carefully treated in calculations of the half-life T_{sf} because they are giving the largest contribution to this half-life. This is due to a large potential energy E and a large inertia B.

D. Fission half-life

A contour map of the logarithm of the fission half-life T_{sf}, given in seconds, is shown in Fig. 7. The structure of the map is similar to that of the barrier height B_f^{dyn} (Fig. 3). One can see that the half-lives are rather large. The largest value, obtained for ^{268}106, is of the order of a few hours (3.5 h). (Larger values are obtained only for transitional nuclei, $N>174$, on the border with the region of spherical superheavy nuclei situated around the nucleus ^{298}114.)

Figure 8 shows the dependence of the logarithm of the fission half-life T_{sf} on the neutron number N, for all considered values of Z. The α-decay half-life T_α is also shown, for completeness. The latter is calculated in the same way as in [2], with small improvements. One can see a clear effect of the $N=162$ shell in the fission half-life T_{sf}, for all Z. The effect is especially strong for $Z=106$. For $Z=104$, also the effect of the lower shell at $N=152$ is visible. The effect of $N=162$, and the smaller effect of $N=152$, are also visible in the α-decay half-life T_α.

The existing experimental values of both T_{sf} and T_α, Fig. 8, are rather well reproduced by the calculations. This

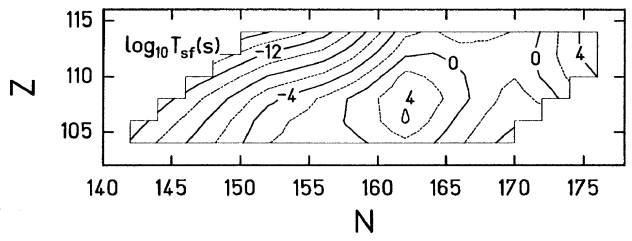

FIG. 7. Same as in Fig. 3, but for the logarithm of the spontaneous-fission half-life T_{sf}, given in seconds.

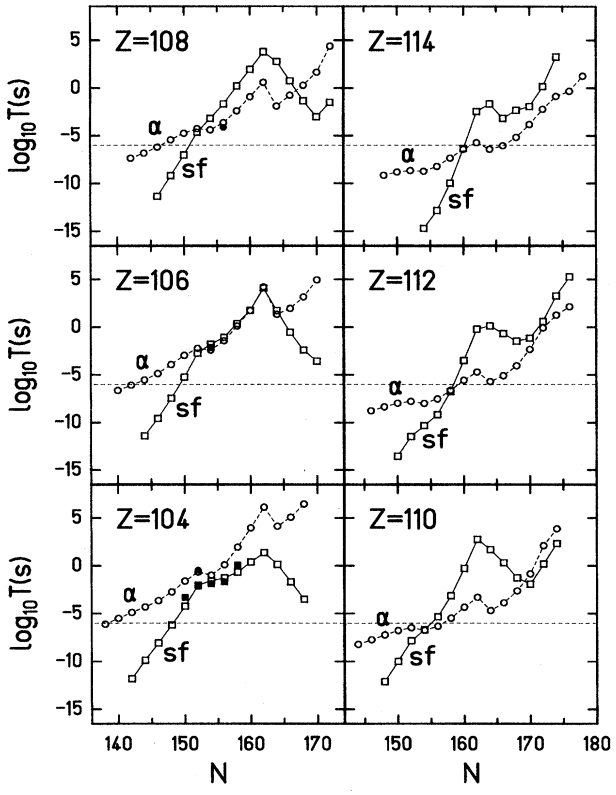

FIG. 8. Dependence of the logarithm of the calculated spontaneous-fission (sf) half-lives, given in seconds, on the neutron number N, for elements 104–114. The α-decay half-lives (α) are also shown, for comparison. Experimental values are given as full symbols. The horizontal dashed line indicates about the lowest half-life (1 μs) of a nucleus, which can be detected in a present-day setup, after its synthesis.

may be considered as a satisfying result as there are no free parameters in the calculations, fitted to experiment.

A comparison between the calculated T_{sf} and T_α shows that, for $Z=104$, T_{sf} is smaller than T_α for all N. For $Z=106$, T_{sf} is comparable with T_α for a large number of isotopes ($N=154-164$). For higher Z, it is even larger than T_α and for an even larger number of isotopes. This seems to be the effect of shells, mainly of that at $N=162$, to which T_{sf} is more sensitive than T_α. Only for the lightest isotopes, T_{sf} is shorter than T_α for all elements investigated.

The results are generally similar to earlier ones [8], obtained in a smaller deformation space. The present values of T_{sf} are significantly lower, however, for $Z=108$ and 110 than the previous ones. This is probably mainly due to the lower values of the dynamical effective inertia, presently used, than those of the phenomenological inertia, exploited previously [8].

More detailed fission properties of the considered nuclei, calculated in this paper, are given in Table I. The first three columns of Table I specify the proton Z, neutron N, and mass A numbers of a nucleus, respectively. The fourth one gives the equilibrium value of the quadrupole component of the deformation β_2^0. This main component of the deforma-

TABLE I. Equilibrium deformation and spontaneous-fission properties of nuclei specified in the first three columns.

Z	N	A	β_2^0	β_2^{en}	β_2^{ex}	B_f^{stat} (MeV)	B_f^{dyn} (MeV)	$\log_{10}T_{sf}(s)$	T_{sf}	T_{sf}^{expt}	Ref.
104	142	246	0.238	0.30	0.56	3.9	4.0	-11.81	1.5 ps		
104	144	248	0.239	0.29	0.57	4.7	4.9	-9.87	0.13 ns		
104	146	250	0.242	0.28	0.58	5.5	5.7	-8.07	8.5 ns		
104	148	252	0.245	0.28	0.60	6.2	6.6	-6.19	.65 μs		
104	150	254	0.248	0.28	0.63	6.7	7.3	-4.22	60 μs	$0.5^{+0.2}_{-0.2}$ ms	[35]
104	152	256	0.249	0.28	0.66	7.0	7.9	-2.04	9.1 ms	$7.4^{+0.9}_{-0.7}$ ms	[36]
104	154	258	0.248	0.27	0.68	6.9	7.9	-1.56	28 ms	13^{+3}_{-3} ms	[37]
104	156	260	0.247	0.27	0.68	6.6	7.8	-1.27	54 ms	21^{+1}_{-1} ms	[37]
104	158	262	0.243	0.27	0.69	6.5	7.6	-0.67	0.21 s	$1.2^{+1.0}_{-0.5}$ s	[17,18]
104	160	264	0.237	0.26	0.69	6.4	7.6	0.39	2.5 s		
104	162	266	0.229	0.26	0.70	6.5	7.8	1.37	23 s		
104	164	268	0.221	0.25	0.69	5.7	6.8	0.14	1.4 s		
104	166	270	0.203	0.24	0.67	4.9	5.4	-1.69	20 ms		
104	168	272	0.196	0.23	0.66	4.2	4.2	-3.50	0.32 ms		
106	144	250	0.239	0.29	0.55	3.9	4.1	-11.40	4.0 ps		
106	146	252	0.242	0.28	0.56	4.6	4.9	-9.56	0.28 ns		
106	148	254	0.244	0.28	0.58	5.3	5.9	-7.45	35 ns		
106	150	256	0.247	0.27	0.62	5.9	6.7	-5.24	5.8 μs		
106	152	258	0.248	0.27	0.66	6.3	7.5	-2.74	1.8 ms		
106	154	260	0.247	0.27	0.68	6.4	7.8	-1.79	16 ms	$7.2^{+4.8}_{-2.7}$ ms	[38]
106	156	262	0.244	0.27	0.69	6.3	7.8	-1.07	85 ms		
106	158	264	0.244	0.26	0.70	6.3	8.1	0.37	2.3 s		
106	160	266	0.239	0.26	0.71	6.4	8.2	1.76	58 s		
106	162	268	0.234	0.25	0.73	6.8	8.8	4.10	3.5 h		
106	164	270	0.225	0.25	0.70	5.9	7.5	1.74	55 s		
106	166	272	0.213	0.25	0.68	5.0	5.9	-0.54	0.29 s		
106	168	274	0.198	0.24	0.67	4.2	4.4	-2.41	3.9 ms		
106	170	276	0.171	0.22	0.66	3.6	3.6	-3.58	0.26 ms		
108	146	254	0.240	0.28	0.54	3.4	3.8	-11.35	4.5 ps		
108	148	256	0.241	0.28	0.56	4.1	4.8	-9.20	0.63 ns		
108	150	258	0.243	0.27	0.59	4.7	5.8	-7.02	95 ns		
108	152	260	0.244	0.27	0.63	5.2	6.4	-4.63	23 μs		
108	154	262	0.243	0.27	0.66	5.4	6.8	-3.18	0.66 ms		
108	156	264	0.242	0.26	0.68	5.5	7.1	-1.67	21 ms		
108	158	266	0.241	0.26	0.70	5.7	7.7	0.21	1.6 s		
108	160	268	0.237	0.26	0.72	6.1	8.0	1.98	1.6 m		
108	162	270	0.233	0.25	0.73	6.5	8.2	3.82	1.8 h		
108	164	272	0.227	0.25	0.71	5.9	7.1	2.82	11 m		
108	166	274	0.217	0.24	0.69	5.1	6.0	0.76	5.8 s		
108	168	276	0.200	0.23	0.68	4.2	4.2	-1.34	46 ms		
108	170	278	0.175	0.22	0.67	3.5	3.5	-3.01	0.98 ms		
108	172	280	0.135	0.19	0.67	3.3	3.3	-1.49	32 ms		
110	148	258	0.236	0.28	0.53	2.6	3.1	-12.11	0.78 ps		
110	150	260	0.237	0.28	0.56	3.2	4.1	-9.99	0.10 ns		
110	152	262	0.241	0.27	0.59	3.7	4.8	-7.83	15 ns		
110	154	264	0.238	0.27	0.62	3.8	5.1	-6.69	0.20 μs		
110	156	266	0.234	0.27	0.64	3.9	5.3	-5.32	4.8 μs		
110	158	268	0.229	0.26	0.66	4.3	5.9	-3.14	0.72 ms		
110	160	270	0.227	0.25	0.68	4.9	6.9	-0.27	0.54 s		
110	162	272	0.226	0.24	0.70	5.6	7.4	2.75	9.4 m		
110	164	274	0.217	0.24	0.69	5.2	6.4	1.68	48 s		

TABLE I. *(Continued).*

Z	N	A	β_2^0	β_2^{en}	β_2^{ex}	B_f^{stat} (MeV)	B_f^{dyn} (MeV)	$\log_{10}T_{sf}(s)$	T_{sf}	T_{sf}^{expt}	Ref.
110	166	276	0.207	0.23	0.68	4.6	5.2	0.32	2.1 s		
110	168	278	0.198	0.22	0.67	4.0	4.0	-1.25	56 ms		
110	170	280	0.153	0.21	0.66	3.5	3.5	-1.92	12 ms		
110	172	282	0.125	0.18	0.66	3.4	3.5	0.19	1.5 s		
110	174	284	0.116	0.15	0.67	3.5	3.6	2.32	3.5 m		
112	150	262	0.232	0.29	0.53	2.0	2.2	-13.55	28 fs		
112	152	264	0.234	0.28	0.56	2.4	2.7	-11.49	3.2 ps		
112	154	266	0.227	0.27	0.58	2.3	2.8	-10.32	48 ps		
112	156	268	0.223	0.27	0.60	2.3	3.0	-9.16	0.69 ns		
112	158	270	0.219	0.26	0.63	2.9	3.8	-6.73	0.19 μs		
112	160	272	0.219	0.25	0.65	3.7	4.5	-3.50	0.32 ms		
112	162	274	0.221	0.24	0.68	4.5	5.9	-0.20	0.63 s		
112	164	276	0.206	0.23	0.67	4.4	4.8	0.13	1.3 s		
112	166	278	0.202	0.22	0.66	4.1	4.1	-0.67	0.21 s		
112	168	280	0.191	0.21	0.65	3.6	3.7	-1.47	34 ms		
112	170	282	0.144	0.19	0.65	3.4	3.5	-1.15	71 ms		
112	172	284	0.123	0.17	0.66	3.4	3.5	0.60	4.0 s		
112	174	286	0.095	0.15	0.66	3.7	4.3	3.29	32 m		
114	154	268	0.219	0.28	0.54	1.2	1.3	-14.71	1.9 fs		
114	156	270	0.209	0.26	0.56	1.3	1.4	-12.84	0.14 ps		
114	158	272	0.207	0.25	0.60	1.7	1.9	-9.98	0.10 ns		
114	160	274	0.208	0.24	0.62	2.5	2.7	-6.34	0.46 μs		
114	162	276	0.212	0.23	0.64	3.4	3.4	-2.46	3.5 ms		
114	164	278	0.203	0.22	0.65	3.6	3.7	-1.66	22 ms		
114	166	280	0.190	0.23	0.65	3.5	3.6	-3.17	0.68 ms		
114	168	282	0.182	0.21	0.64	3.2	3.4	-2.33	4.7 ms		
114	170	284	0.143	0.19	0.64	3.1	3.3	-1.93	12 ms		
114	172	286	0.121	0.17	0.65	3.3	3.8	0.17	1.5 s		
114	174	288	0.086	0.14	0.66	4.1	4.7	3.32	35 m		

tion of a nucleus is chosen to parametrize the position of a point on the fission trajectory. Columns 5 and 6 give the entrance and exit points to and from the barrier, respectively, and columns 7 and 8 give the heights of the static and dynamic barriers. The logarithm of the fission half-life (given in seconds), $\log_{10}T_{sf}(s)$, is presented in column 9 and the half-life itself in column 10. Columns 11 and 12 give experimental values of T_{sf} and the respective references.

One can see in Table I that the theoretical values reproduce the experimental results rather well, within a factor of 3, on the average. The largest discrepancy is obtained for nucleus ^{254}104, for which the theoretical value is smaller than the experimental one by a factor of 8. Preliminary results of more recent measurements [39] give, however, a value [40] which is closer to the calculated value.

It is interesting to check how well the experimental half-lives of lighter elements with $Z=102$ and 100 are reproduced. This can be done, however, for only these nuclei, for which our deformation space is sufficient to describe their fission. These are the following nuclei: ^{258,260,262}102 and ^{258}100. The calculated T_{sf} for them are 26 ms, 34 ms, 130 ms, and 8.9 ms, respectively, and the measured ones (1.2 $\pm$0.2) ms [14], 100 ms [37], 5 ms [41], and (370$\pm$43)μs [42], respectively. One can see that the discrepancies between the calculated and measured values are similar to those obtained for nuclei of heavier elements with $Z=104$ and 106.

A comparison of our half-lives with other calculated values, those of [9], shows that those values are smaller than ours by up to about eight orders of magnitude. Also the results of [10,43] are very different from ours. For nuclei with neutron number N close to the magic value $N=162$, the half-lives T_{sf} of [10,43] are smaller than ours by up to more than six orders of magnitude. The difference seems to originate mainly from smaller phenomenologic inertia taken in [9,10,43] than the microscopic inertia obtained in this paper.

One can see in Table I that almost all considered nuclei are well deformed (large β_2^0). Only the heaviest isotopes, especially those of the elements with largest Z, are transitional. The barriers are thin, especially those of the most neutron-deficient isotopes. Some of these barriers end at quite small deformations $\beta_2 \approx 0.55$–0.60. The static fission

barrier is systematically lower than the dynamical one by up to about 2 MeV.

E. Sensitivity of calculated fission half-life to various factors

It is known that the fission half-life T_{sf} is very sensitive to changes of various quantities appearing in the calculations. It is because most of these quantities (height of the potential-energy barrier, its width and generally shape, effective inertia) appear in the exponent. Because of this, a sensitivity to changes of these quantities and to changes in an applied approach which modify them is often discussed. For example, the whole of Ref. [32] has been devoted to a discussion of the role of the deformation space admitted in the analysis of spontaneous fission. The discussion has been performed for the nucleus $^{260}106$, which is the heaviest even-even nucleus with measured T_{sf}. It has been found that the analysis performed in three-dimensional deformation space $\{\beta_\lambda\}$, $\lambda=2,4,6$, leads to T_{sf} larger by about three orders of magnitude than T_{sf} obtained in two-dimensional space $\{\beta_\lambda\},\lambda=2,4$. The inclusion of the fourth dimension β_8 increases T_{sf}, however, by only about half of the order of magnitude.

Here, we will illustrate the sensitivity of T_{sf} to changes of the zero-point energy E_{zp}, Eq. (9). As mentioned in Sec. II E, the value $E_{zp}=0.7$ MeV has been taken in the present calculations. It is close to the result of [2], where it has been obtained in the adiabatic and harmonic approximations from the potential energy and the inertia tensor, both calculated in the same way as in the present paper. The calculation was rather simplified, and the value cannot be considered as very well established. So an examination of the uncertainty in T_{sf}, coming from an uncertainty in E_{zp}, is reasonable.

To be close rather to the upper than to the lower limit of the sensitivity, we choose, for the discussion, the nucleus $^{268}106$, which has the largest T_{sf} of all nuclei studied in the present paper. We find that the increase of $E_{zp}=0.7$ MeV by 0.2 MeV decreases T_{sf} by about 0.9 of the order of magnitude, while the decrease of it by 0.2 MeV increases T_{sf} by about 1.5 of the order of magnitude.

The sensitivity to the zero-point energy is also a sensitivity to the height of the fission barrier. It may be also translated to the sensitivity to the average value of the inertia. Thus, it gives an idea of the sensitivity of T_{sf} to various factors appearing in the calculation of it.

To get an idea of numerical errors coming from the approximations to the fisson trajectory and to the action integral along this trajectory, we changed the density of the grid points in both β_2 and β_4. We found that with $\Delta\beta_2$ decreasing from 0.025 to 0.010 and $\Delta\beta_4$ from 0.010 to 0.0025 (cf. Sec. II E), $\log_{10}T_{sf}(s)$ was increasing continuously from 3.3 to 4.1, for the case of $^{268}106$. With a further decrease of $\Delta\beta_2$ and $\Delta\beta_4$, $\log_{10}T_{sf}(s)$ was fluctuating around the value 4.1 with an amplitude of about 0.1. A more detailed discussion of numerical errors in calculations of T_{sf} has been recently performed in [44]. The discussion has been restricted, however, to only one-dimensional deformation space. Thus, it does not include errors connected with the determination of the fission trajectory.

F. Remark on terminology

It seems to be practical to have some name for the very specific region of nuclei considered in the present paper, due to its specifics and also to a large recent activity, both experimental and theoretical, in the study of these nuclei. The name "deformed superheavy nuclei" is a rather natural possibility. It has already been used for some time [45]. It makes use of the suggestion of Armbruster [46,47] to extend the name "superheavy nuclei," primarily reserved [48] for spherical nuclei around the hypothetical doubly magic nucleus $^{298}114$, to all nuclei with very large Z and N, which exist or are expected to exist only due to their shell effects. Recent calculations indicate that the discussed nuclei fulfill this condition. The adjective "deformed" reflects their expected shape and distinguishes them from the "traditional" superheavy nuclei around $^{298}114$, which should be called "spherical superheavy nuclei." Such a distinction could not be made by the names of elements, as some isotopes of a given element [e.g., 108 (Hs) or 109 (Mt)] belong to one (e.g., deformed) and others to the second (spherical) region of nuclei.

At least for a part of the discussed region of nuclei, the name "rock" [43] has been also proposed, in connection with their increased stability.

IV. CONCLUSIONS

The following conclusions may be drawn from the present study.

(1) Almost all considered nuclei are predicted to be deformed. Only very few of them, the heaviest ones, are expected to be transitional.

(2) The ground-state fission barriers of the nuclei are thin. They already end at deformations $\beta_2\approx 0.55$–0.70.

(3) The barriers are, however, high. For about 20 of the considered nuclei, the dynamical fission barrier is higher than 7 MeV. The largest value, 8.8 MeV, is obtained for the nucleus $^{268}106$ (^{268}Sg), i.e., the nucleus with the predicted closed neutron shell at $N=162$. The static barriers are by up to about 2 MeV lower than the dynamical ones.

(4) The large height of the fission barrier is mainly due to a large shell correction to the ground-state energy of these nuclei. The largest (negative) value of this correction, -7.2 MeV, is obtained for the nucleus $^{270}108$ (^{270}Hs), predicted to be a doubly magic deformed nucleus.

(5) Because of high barriers, the spontaneous-fission half-lives T_{sf} of the considered nuclei are rather large. The largest value, 3.5 h, is obtained for the nucleus $^{268}106$.

(6) The existing experimental values of T_{sf}, for nuclei in the considered region, are rather well reproduced by the calculations.

(7) A comparison between the calculated fission, T_{sf}, and α-decay, T_α, half-lives shows that, for $Z=104$, T_{sf} is smaller than T_α, $T_{sf}<T_\alpha$, for all N. For $Z=106$, $T_{sf}\approx T_\alpha$ for a large number of isotopes ($N=154$–164). For higher Z, T_{sf} is even larger than T_α and for even a larger number of isotopes. Only for the most neutron-deficient isotopes of the considered elements T_{sf} is smaller than T_α.

(8) Thus, the results show that many nuclei, not yet observed, in the considered region are expected to have sufficiently long half-lives to be observed in a present-day experimental setup, if synthesized.

ACKNOWLEDGMENTS

The authors would like to thank Peter Armbruster, Sigurd Hofmann, Gottfried Münzenberg, Wolfgang Nörenberg, and

Matthias Schädel for many valuable discussions and suggestions. They are also grateful to D.C. Hoffman, E.K. Hulet, Yu.A. Lazarev, R.W. Lougheed, V. Ninov, Yu.Ts. Oganessian, Z. Patyk, A.G. Popeko, W. Reisdorf, P. Rozmej, S. Saro, and A.V. Yeremin for helpful discussions. Support by the Polish Committee for Scientific Research (KBN), Grant No. 2 P03B 156 08, and by GSI-Darmstadt is gratefully acknowledged.

[1] Z. Patyk and A. Sobiczewski, Phys. Lett. B **256**, 307 (1991).
[2] Z. Patyk and A. Sobiczewski, Nucl. Phys. **A533**, 132 (1991).
[3] Z. Patyk, A. Sobiczewski, P. Armbruster, and K.-H. Schmidt, Nucl. Phys. **A491**, 267 (1989).
[4] A. Baran, K. Pomorski, S.E. Larsson, P. Möller, S.G. Nilsson, J. Randrup, and A. Sobiczewski, in Proceedings of the 3rd International Conference on Nuclei Far From Stability, Cargèse, 1976, Report No. CERN 76-13, Geneva, 1976 (unpublished), p. 537.
[5] A. Baran, K. Pomorski, A. Lukasiak, and A. Sobiczewski, Nucl. Phys. **A361**, 83 (1981).
[6] Z. Patyk, J. Skalski, A. Sobiczewski, and S. Ćwiok, Nucl. Phys. **A502**, 591c (1989).
[7] J. Randrup, S.E. Larsson, P. Möller, S.G. Nilsson, K. Pomorski, and A. Sobiczewski, Phys. Rev. C **13**, 229 (1976).
[8] K. Böning, Z. Patyk, A. Sobiczewski, and S. Ćwiok, Z. Phys. A **325**, 479 (1986).
[9] P. Möller, J.R. Nix, and W.J. Swiatecki, Nucl. Phys. **A469**, 1 (1987).
[10] P. Möller, J.R. Nix, and W.J. Swiatecki, Nucl. Phys. **A492**, 349 (1989).
[11] S. Ćwiok and A. Sobiczewski, Z. Phys. A **342**, 203 (1992).
[12] G. Münzenberg, Rep. Prog. Phys. **51**, 57 (1988).
[13] D.C. Hoffman and L.P. Somerville, in *Particle emission from nuclei*, edited by D.N. Poenaru and M.S. Ivascu (CRC Press, Boca Raton, 1989), Vol. 3, p. 1.
[14] E.K. Hulet, J.F. Wild, R.J. Dougan, R.W. Lougheed, J.H. Landrum, A.D. Dougan, P.A. Baisden, C.M. Henderson, R.J. Dupzyk, R.L. Hahn, M. Schädel, K. Sümmerer, and G.R. Bethune, Phys. Rev. C **40**, 770 (1989).
[15] G.T. Seaborg and W.D. Loveland, *The Elements Beyond Uranium* (Wiley, New York, 1990).
[16] S. Hofmann, in *Proceedings of the International Conference on Actinides-93,* Santa Fe, 1993 [J. Alloys Comp. **213/ 214**, 74 (1994)].
[17] R.W. Lougheed, K.J. Moody, J.F. Wild, E.K. Hulet, J.H. McQuaid, Yu.A. Lazarev, Yu.V. Lobanov, Yu.Ts. Oganessian, V.K. Utyonkov, F.Sh. Abdullin, G.V. Buklanov, B.N. Gikal, S. Iliev, A.N. Mezentsev, A.N. Polyakov, I.M. Sedykh, I.V. Shirokovsky, V.G. Subbotin, A.M. Sukhov, Yu.S. Tsyganov, and V.E. Zhuchko, in *Proceedings of the International Conference on Actinides-93,* Santa Fe, 1993 [J. Alloys Comp. **213/ 214**, 61 (1994)].
[18] Yu.A. Lazarev, Yu.V. Lobanov, Yu.Ts. Oganessian, V.K Utyonkov, F.Sh. Abdullin, G.V. Buklanov, B.N. Gikal, S. Iliev, A.N. Mezentsev, A.N. Polyakov, I.M. Sedykh, I.V. Shirokovsky, V.G. Subbotin, A.M. Sukhov, Yu.S. Tsyganov, V.E. Zhuchko, R.W. Lougheed, K.J. Moody, J.F. Wild, E.K. Hulet, and J.H. McQuaid, Phys. Rev. Lett. **73**, 624 (1994).
[19] P. Armbruster, in *Proceedings of the International Conference on Nuclear Shapes and Nuclear Structure at Low Excitation Energies*, Antibes, France, 1994, edited by M. Vergnes, D. Goutte, P.H. Heenen, and J. Sauvage (Editions Frontieres, Gif-sur-Yvette, 1994), p. 365.
[20] R. Smolańczuk, J. Skalski, and A. Sobiczewski, in *Proceedings of the International School-Seminar on Heavy Ion Physics*, Dubna, Russia, 1993, edited by Yu.Ts. Oganessian, Yu.E. Penionzhkevich, and R. Kalpakchieva (JINR, Dubna, 1993), Vol. 1, p. 157.
[21] R. Smolańczuk, J. Skalski, and A. Sobiczewski, in *Frontier Topics in Nuclear Physics*, edited by W. Scheid and A. Sandulescu, Vol. 334 of Advanced Study Institue, NATO Series B: Physics (Plenum Press, New York, 1994), p. 151.
[22] A. Sobiczewski, R. Smolańczuk, and J. Skalski, in *Proceedings of the International Conference on Actinides-93,* Santa Fe, 1993 [J. Alloys Comp. **213/ 214**, 38 (1994)].
[23] H.J. Krappe, J.R. Nix, and A.J. Sierk, Phys. Rev. C **20**, 992 (1979).
[24] P. Möller and J.R. Nix, Nucl. Phys. **A361**, 117 (1981); At. Data Nucl. Data Tables **26**, 165 (1981).
[25] S. Ćwiok, J. Dudek, W. Nazarewicz, J. Skalski, and T. Werner, Comput. Phys. Commun. **46**, 379 (1987).
[26] A. Sobiczewski, Z. Szymański, S. Wycech, S.G. Nilsson, J.R. Nix, C.F. Tsang, P. Möller, and B. Nilsson, Nucl. Phys. **A131**, 67 (1969).
[27] M. Brack, J. Damgaard, A.S. Jensen, H.C. Pauli, V.M. Strutinsky, and C.Y. Wong, Rev. Mod. Phys. **44**, 320 (1972).
[28] K. Pomorski, T. Kaniowska, A. Sobiczewski, and S.G. Rohoziński, Nucl. Phys. **A283**, 394 (1977).
[29] A. Sobiczewski, Sov. J. Part. Nucl. **10**, 1170 (1979).
[30] H.C. Pauli, Phys. Rep. C **7**, 35 (1973); Nukleonika **20**, 601 (1975).
[31] S.E. Larsson, Phys. Scr. **8**, 17 (1973).
[32] R. Smolańczuk, H.V. Klapdor-Kleingrothaus, and A. Sobiczewski, Acta Phys. Pol. B **24**, 685 (1993).
[33] A. Sobiczewski, Z. Patyk, S. Ćwiok, and P. Rozmej, Nucl. Phys. **A485**, 16 (1988).
[34] M. Schädel (private communication).
[35] G.M. Ter-Akopyan, A.S. Iljinov, Yu.Ts. Oganessian, O.A. Orlova, G.S. Popeko, S.P. Tretyakova, V.I. Chepigin, B.V. Shilov, and G.N. Flerov, Nucl. Phys. A **255**, 509 (1975).
[36] F.P. Hessberger, G. Münzenberg, S. Hofmann, W. Reisdorf, K.H. Schmidt, H.J. Schött, P. Armbruster, R. Hingmann, B. Thuma, and D. Vermeulen, Z. Phys. A **321**, 317 (1985).
[37] L.P. Somerville, M.J. Nurmia, J.M. Nitschke, A. Ghiorso, E.K. Hulet, and R.W. Lougheed, Phys. Rev. C **31**, 1801 (1985).
[38] G. Münzenberg, S. Hofmann, H. Folger, F.P. Hessberger, J. Keller, K. Poppensieker, B. Quint, W. Reisdorf, K.H. Schmidt, H.J. Schött, P. Armbruster, M.E. Leino, and R. Hingmann, Z. Phys. A **322**, 227 (1985).
[39] S. Hofmann *et al.* (unpublished).
[40] S. Hofmann (private communication).
[41] E.K. Hulet, in Proceedings of the Robert A. Welch Foundation Conference on Chemical Research XXXIV "Fifty Years with

Transuranium Elements," Houston, 1990 (unpublished), p. 279.
[42] E.K. Hulet, R.W. Lougheed, J.F. Wild, R.J. Dougan, K.J. Moody, R.L. Hahn, C.M. Henderson, R.J. Dupzyk, and G.R. Bethune, Phys. Rev. C **34**, 1394 (1986).
[43] P. Möller and J.R. Nix, J. Phys. G **20**, 1681 (1994).
[44] A. Baran and Z. Lojewski, Acta Phys. Pol. B **25**, 621 (1994).
[45] A. Sobiczewski, Z. Patyk, and S. Ćwiok, Phys. Lett. B **224**, 1 (1989).
[46] P. Armbruster, Annu. Rev. Nucl. Part. Sci. **35**, 135 (1985).
[47] P. Armbruster, in *Proceedings of the International School on Heavy Ion Physics*, Erice, Italy, 1986, edited by R.A. Broglia and G.F. Bertsch (Plenum Press, New York, 1988), p. 153.
[48] W.D. Myers and W.J. Swiatecki, Nucl. Phys. **81**, 1 (1966).